

ERB-703

UNCLASSIFIED

NATIONAL RESEARCH COUNCIL OF CANADA
RADIO AND ELECTRICAL ENGINEERING DIVISION

FREE - FLOATING METALLIZED PLASTIC BALLOONS
FOR USE AS RADAR TARGETS

A. HENDRY AND J. AKEROYD

OTTAWA
APRIL 1965

ABSTRACT

The use of free-floating metallized plastic balloons for radar performance evaluation is described. The balloons, fabricated from aluminized Mylar, are four feet in diameter, and float at altitudes of the order of 40,000 feet. The relationship of stability of the equilibrium to superpressure and to solar heating is discussed. Experimental results of bursting tests and microwave reflectivity are included, along with a brief summary of experimental results and flight trials.

CONTENTS

	<u>Page</u>
Introduction	1
Buoyancy of Free Balloons	2
Stability of Free Balloons	4
Bursting Stress of Spherical Plastic Balloons	8
Radar Cross Section and Reflectivity of Metallized Plastic Balloons	9
Flight Characteristics of Various Balloon Assemblies	12
Experimental Results	14
Acknowledgment	15
Sources of Atmospheric Data	16
References	16

FIGURES

1. Mean atmospheric density versus altitude
2. $Q\rho_{Go}$ versus altitude for helium
3. Mean atmospheric temperature versus altitude
4. $Q'\rho_{Go}$ versus altitude for helium
5. Temperature stability factor for superpressured balloons
6. ΔP versus diameter for 7500 psi stress in 1-mil spherical balloons
7. Calculated reflectivity of aluminum film in RG48/U waveguide at 3.0 Gc/s
8. Calculated equilibrium altitudes for spherical balloons

LIST OF SYMBOLS

F	force
g	acceleration due to gravity
h	altitude
K	constant of proportionality (See Eq. 15)
M	mass
M_A	mass of accessories
M_B, m_B	mass of balloon
M_G	mass of gas fill
M_{Go}	mass of gas fill at sea level
M_v	mass of valve
n	quantity of gas, moles
P_a	atmospheric pressure
P_{ao}	sea-level atmospheric pressure
ΔP	balloon superpressure
Q	See Eq. (9)
Q'	See Eq. (25)
R	ideal gas constant, radius of the earth
r	balloon radius
S	stress
t	balloon thickness
T_a	atmospheric temperature
T_{ao}	sea-level atmospheric temperature
T_G	temperature of gas in balloon
ΔT	maximum tolerable solar heating
V, v	volume of balloon
W	weight of balloon assembly
ρ_a	atmospheric density
ρ_{ao}	sea-level atmospheric density
ρ_B	"density" of balloon assembly
ρ_{Go}	sea-level density of gas fill

FREE-FLOATING METALLIZED PLASTIC BALLOONS

FOR USE AS RADAR TARGETS

- A. Hendry and J. Akeroyd -

INTRODUCTION

For radar performance evaluation, spherical, free-floating plastic balloons offer many advantages. Such balloons maintain their size and shape as long as the internal pressure exceeds that of the surrounding atmosphere; hence they provide a constant and calculable radar cross section. These balloons, which are launched in such a way that atmospheric winds will carry them through the area covered by the radar, attain high altitudes, and subsequently drift at approximately constant altitude out to the maximum range of the radar.

From the observed maximum range of the radar, the over-all performance of the radar may be inferred. If a balloon is within the coverage of two or more radars simultaneously, a comparison of the height and location readings provides a valuable check on the accuracy of registration. The relatively slow speed of wind-borne balloons is advantageous in making such comparisons.

In areas where high-altitude aircraft are infrequently observed, routine performance checks using balloons are likely to be much less expensive than similar tests using aircraft, if the flights must be made solely to provide radar targets. The constant echoing area of the balloons simplifies the task of interpreting data obtained from test flights. Although the heading and speed of the balloon cannot be varied at will, these limitations are partly offset by the advantage that balloons may be launched from any accessible area, and therefore airport facilities are not required.

The prime requirement for radar target balloons is sustained level flight at a predetermined altitude. The flight must be of such length that the wind-borne balloon will pass out of the radar coverage area; hence level flight for 10 hours has been chosen as a design goal. Altitudes of 40,000 to 100,000 feet are of interest. For such heights, using commercially available plastic balloons, diameters of 4 to 25 feet are required. The standard echoing area chosen is that of a metallized plastic balloon, 4 feet in diameter. For the lower altitudes, the echoing balloon alone is sufficient, while for higher altitudes, a lifting balloon which is unmetallized and of larger diameter, must be used. The metal coating used on these balloons is vacuum-deposited aluminum, of the order of 400 angstrom units in thickness. This coating reflects over 97% of the incident energy in the microwave region. There is no significant difference in weight between the metallized and unmetallized plastic, since the coating is so thin. The balloons are equipped with valves which vent excess gas, and thereby prevent the internal pressure from exceeding atmospheric pressure by more than a preset amount.

BUOYANCY OF FREE BALLOONS

A balloon immersed in a gas of density ρ_a experiences a buoyancy force given by:

$$F = V\rho_a g, \quad (1)$$

where V is the volume of the balloon, and g is the acceleration of gravity. This force is opposed by the weight W of the balloon assembly.

$$W = (M_B + M_V + M_G + M_A)g, \quad (2)$$

where

- M_B = mass of balloon material,
- M_V = mass of valve mechanism,
- M_G = mass of gas fill,
- M_A = mass of accessories or payload.

The equilibrium altitude is that for which $F = W$. For a valved balloon, i.e., one from which gas is expelled as the balloon rises, M_G is a function of altitude. To obtain the equilibrium altitude, it is necessary to relate M_G to altitude. This may be done as follows, assuming that the ideal gas law holds; i.e., that

$$PV = nRT, \quad (3)$$

where n is the number of moles of gas.

Assume that the balloon is initially filled at sea level to atmospheric pressure, plus a pressure differential ΔP which is the valve setting. (This is probably the most practical method of filling for small balloons. It provides a check on the balloon and valve at the time of release, and will also provide high net lift, thus minimizing the time required for ascent to altitude.) At sea level, the mass of the gas fill is:

$$M_{Go} = \left(\frac{P_{ao} + \Delta P}{P_{ao}} \right) \rho_{Go} V, \quad (4)$$

where P_{ao} = sea-level atmospheric pressure,
 ρ_{Go} = sea-level density of the gas fill.

As the balloon rises, the atmospheric pressure and temperature change. If it is assumed that the ascent is made sufficiently slowly so that the internal pressure is always $P_a + \Delta P$, and the internal temperature is T_a , where P_a and T_a are the pressure and temperature, respectively, of the atmosphere, the mass of the gas fill will be:

$$M_G = \left(\frac{P_a + \Delta P}{P_{a0} + \Delta P} \right) \left(\frac{T_{a0}}{T_a} \right) M_{G0} . \quad (5)$$

Combining (4) and (5),

$$M_G = \left(\frac{T_{a0}}{T_a} \right) \left(\frac{P_a + \Delta P}{P_{a0}} \right) \rho_{G0} V . \quad (6)$$

Thus the net lift is:

$$F - W = V \rho_a g - \left[\left(\frac{T_{a0}}{T_a} \right) \left(\frac{P_a + \Delta P}{P_{a0}} \right) \rho_{G0} V + M_B + M_V + M_A \right] g . \quad (7)$$

It is convenient to write this as follows:

$$F - W = V \rho_a g - \left[V Q \rho_{G0} + M_B + M_V + M_A \right] g , \quad (8)$$

where for brevity, Q has been defined as follows:

$$Q = \left(\frac{T_{a0}}{T_a} \right) \left(\frac{P_a + \Delta P}{P_{a0}} \right) . \quad (9)$$

Note that Q depends only upon the properties of the atmosphere, and upon the valve setting, ΔP . Although (8) may be used directly for determining the equilibrium altitude, it is more useful, if various balloon sizes are being considered, to reduce the terms to densities; i.e.,

$$\frac{F - W}{Vg} = \rho_a - \left(Q \rho_{G0} + \rho_B \right) , \quad (10)$$

where ρ_B , the pseudo-density of the balloon, is computed as follows:

$$\rho_B = \frac{M_B + M_V + M_A}{V} \quad (11)$$

(Note that V must be the fully inflated volume of the balloon.)

By setting the left-hand side of (10) equal to zero, the condition for equilibrium is obtained in this concise form:

$$Q\rho_{Go} + \rho_B = \rho_a . \quad (12)$$

This is easily solved graphically by finding the altitude at which ρ_a exceeds $Q\rho_{Go}$ by the amount ρ_B .

The equilibrium altitude may be determined by plotting $Q\rho_{Go}$ and ρ_a vs. altitude to the same scale. If the plot of $Q\rho_{Go}$ is prepared on a transparent sheet, and used as an overlay over the plot of ρ_a , then by setting the origin of the first curve over a density corresponding to the value of ρ_B on the plot of ρ_a , the altitude at which the two curves intersect will be the equilibrium altitude. This method has been incorporated into a calculator shown in Plate I.

Fig. 1 is a plot of ρ_a vs. altitude. $Q\rho_{Go}$ is plotted in Fig. 2 for helium as the lifting gas with ΔP as a parameter.

STABILITY OF FREE BALLOONS

To achieve stable (i.e., constant altitude) flight with a free-flying balloon, it is necessary to use constant-volume balloons operating with superpressure; i.e., the internal pressure must exceed the atmospheric pressure at the equilibrium altitude. Underinflated balloons are unstable except under special circumstances.

Consider first the flight of a partially inflated balloon. From equations (1) and (3) the lift force, which is a function of altitude, is given by:

$$F = \frac{\rho_a g n R T_G}{P_a} , \quad (13)$$

where n is the number of moles of gas enclosed and T_G is its temperature. Since the weight of the balloon assembly is fixed, the stability of equilibrium depends upon the variation of F with altitude. At equilibrium,

$$F - W = 0 . \quad (14)$$

For this equilibrium condition to be stable, $\frac{dF}{dh}$ must be negative, so that any deviation from the equilibrium altitude will cause a restoring force. If $\frac{dF}{dh}$ is positive, the equilibrium will be unstable, while if $\frac{dF}{dh}$ is zero, a condition of neutral equilibrium will occur, and the balloon will drift randomly in altitude.

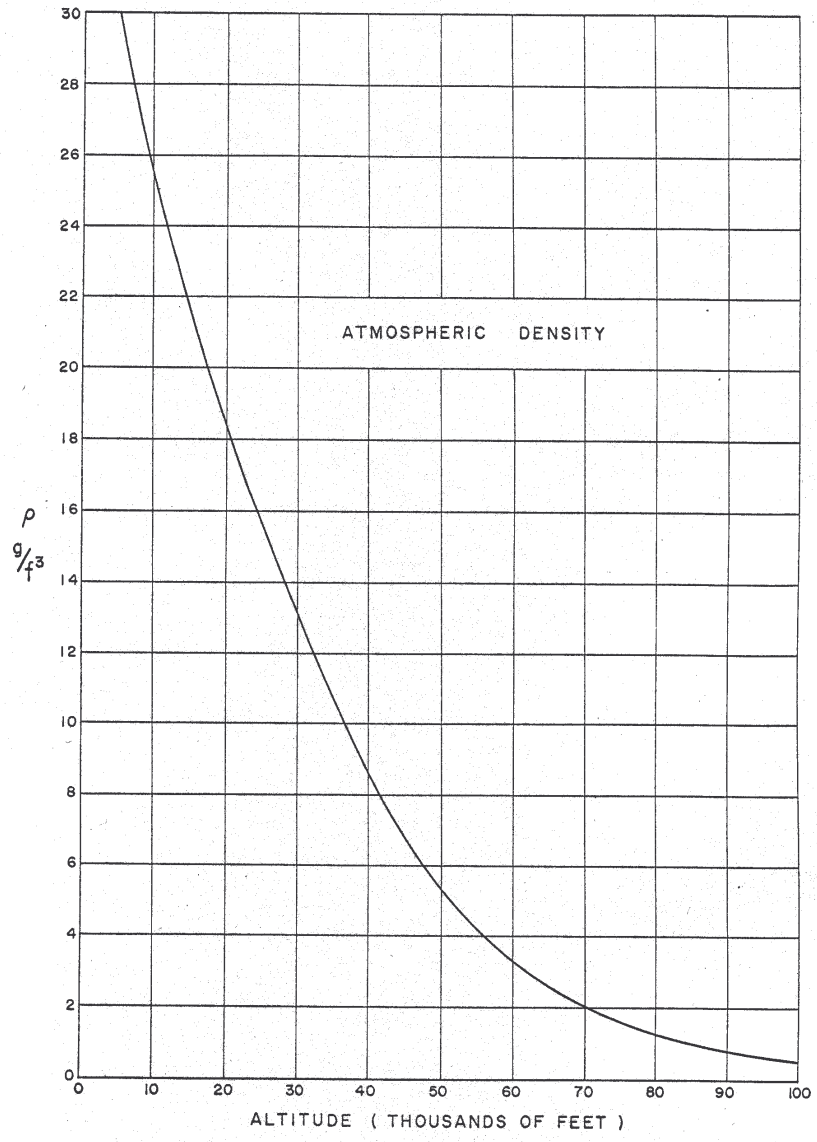


Fig. 1 Mean atmospheric density versus altitude

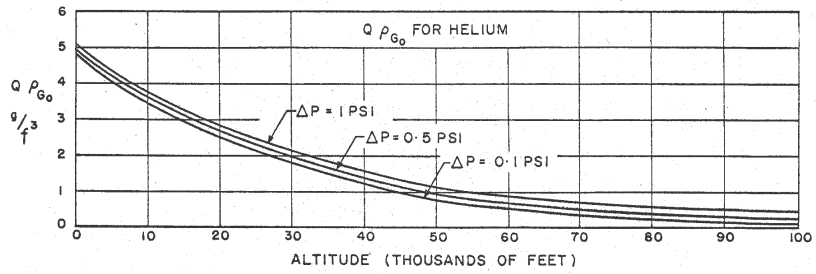


Fig. 2 $Q \rho_{G_0}$ versus altitude for helium

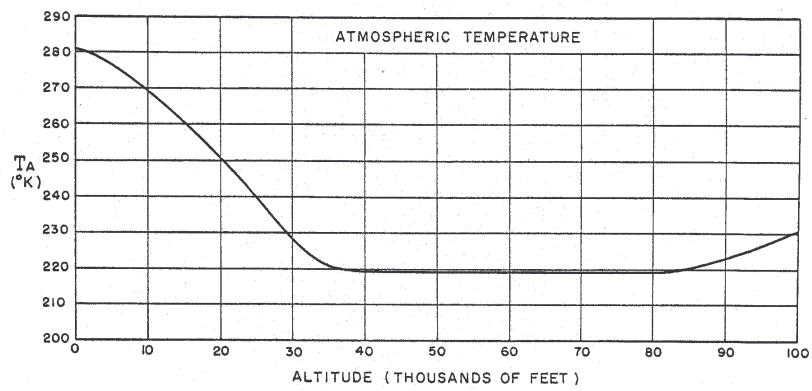


Fig. 3 Mean atmospheric temperature versus altitude

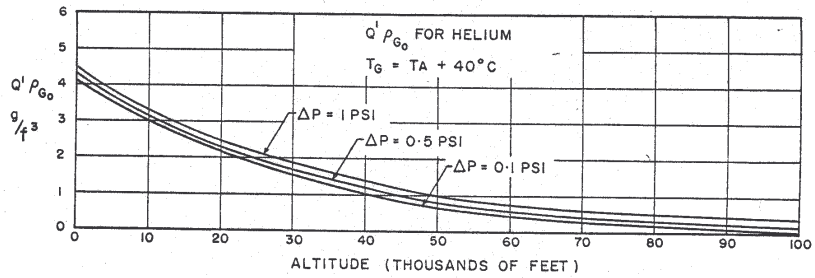


Fig. 4 $Q' \rho_{G_0}$ versus altitude for helium

Since

$$P_a = K \rho_a T_a \quad (15)$$

where K is some constant of proportionality, (13) may be written:

$$F = \frac{g n R T_G}{K T_a} \quad (16)$$

Using

$$\frac{dF}{dh} = \frac{\partial F}{\partial T_G} \frac{dT_G}{dh} + \frac{\partial F}{\partial T_a} \frac{dT_a}{dh},$$

$$\frac{dF}{dh} = \frac{g n R}{K} \left(\frac{1}{T_a} \frac{dT_G}{dh} - \frac{T_G}{T_a^2} \frac{dT_a}{dh} \right) \quad (17)$$

If $T_G = T_a$, which would normally be the case during darkness, the quantity in brackets is zero, and neutral equilibrium will occur.

It is of interest to see under what conditions a stable flight of a partially inflated balloon could be made.

If we assume $\frac{dT_G}{dh} = \frac{dT_a}{dh}$, corresponding to a constant temperature difference between T_G and T_a with varying altitude, (17) becomes:

$$\frac{dF}{dh} = \frac{g n R}{K} \left(\frac{T_a - T_G}{T_a^2} \right) \frac{dT_a}{dh} \quad (18)$$

Thus stable equilibrium could be achieved if $T_G < T_a$, when $\frac{dT_a}{dh}$ is negative, and also, if $T_G > T_a$, when $\frac{dT_a}{dh}$ is positive. The sign of $\frac{dT_a}{dh}$ may be determined from Fig. 3 which is a plot of T_a vs. altitude. Thus from sea level up to approximately 35,000 feet, in which region $\frac{dT_a}{dh}$ is negative, and above approximately 85,000 feet, where $\frac{dT_a}{dh}$ is positive, stable flights could be achieved. Between these two altitudes, however, $\frac{dT_a}{dh}$ is nearly zero, and stable equilibrium of a partially filled balloon is not achievable.

For a superpressure balloon, i.e., an inextensible balloon which is completely filled, the stability of equilibrium may be determined from equation (10):

$$\frac{1}{V_g} \frac{dF}{dh} = \frac{d\rho_a}{dh} - \rho_{Go} \frac{dQ}{dh} \quad (19)$$

From (9)

$$\frac{dQ}{dh} = \left(\frac{T_{ao}}{T_a} \right) \left(\frac{1}{P_{ao}} \right) \left(\frac{dP_a}{dh} \right) - \left(\frac{P_a + \Delta P}{P_{ao}} \right) \left(\frac{T_{ao}}{T_a^2} \right) \left(\frac{dT_a}{dh} \right) \quad (20)$$

Using (15)

$$\frac{dP_a}{dh} = K T_a \frac{d\rho_a}{dh} + K \rho_a \frac{dT_a}{dh} \quad (21)$$

Simplifying,

$$\frac{1}{V_g} \frac{dF}{dh} = \left[1 - \left(\frac{\rho_{Go} T_{ao}}{P_{ao}} \right) \left(\frac{P_a}{\rho_a T_a} \right) \right] \frac{d\rho_a}{dh} - \rho_{Go} \left[\frac{2P_a T_{ao} + \Delta P T_{ao}}{P_{ao} T_a^2} \right] \frac{dT_a}{dh} \quad (22)$$

As $\frac{P_a}{\rho_a T_a}$ is a constant (see (15)), and since $\left(\frac{\rho_{Go} T_{ao}}{P_{ao}} \right)$ is constant, if the quantity in the first bracket is positive at sea level, it will be positive throughout the atmosphere. At sea level, the quantity in brackets is $\left[1 - \frac{\rho_{Go}}{\rho_{ao}} \right]$. Since a prerequisite for the lifting gas is that $\rho_{Go} < \rho_{ao}$, this quantity is positive. Because $\frac{d\rho_a}{dh}$ is always negative, the first term in (22) is always negative. Thus $\frac{dF}{dh}$ is negative, and stability is possible for regions of the atmosphere where $\frac{dT_a}{dh}$ is zero or positive; i.e., above roughly 35,000 feet.

Below this altitude, $\frac{dT_a}{dh}$ is negative, and the second term of (22) becomes positive; however, the second term is too small to make $\frac{dF}{dh}$ positive. This may be seen by direct comparison of $\frac{d\rho_a}{dh}$ and $\rho_{Go} \frac{dQ}{dh}$ (see (19)), being, respectively, the slopes of the curves plotted in Figs. 1 and 2. Note that $\frac{d\rho_a}{dh}$ is more negative than is $\rho_{Go} \frac{dQ}{dh}$; hence dF/dh is negative. Thus stable equilibrium of a super-pressure balloon is possible throughout the atmosphere.

A different type of instability, which may occur with valved balloons, is a result of solar heating. Consider a stable balloon with no solar radiation. At equilibrium:

$$V\rho_a - \left[\left(\frac{T_{a0}}{T_a} \right) \left(\frac{P_a + \Delta P}{P_{a0}} \right) \rho_{G0} V + (M_B + M_v + M_A) \right] = 0. \quad (23)$$

When solar heating occurs, the internal gas temperature rises. Since the pressure differential is fixed, gas will be expelled, and the balloon will rise until a new equilibrium is reached, where

$$V\rho_a - \left[\left(\frac{T_{a0}}{T_G} \right) \left(\frac{P_a + \Delta P}{P_{a0}} \right) \rho_{G0} V + (M_B + M_v + M_A) \right] = 0. \quad (24)$$

If we define

$$Q' = \left(\frac{T_{a0}}{T_G} \right) \left(\frac{P_a + \Delta P}{P_{a0}} \right), \quad (25)$$

(compare with (9)) curves of $Q'\rho_{G0}$ may be used, in the same manner that the curve of $Q\rho_{G0}$ was used to find the new equilibrium altitude. Such a curve is given in Fig. 4, where a 40°C temperature rise due to solar heating was assumed.

Upon the cessation of solar heating (i.e., at sunset) the balloon will cool to atmospheric temperature, and its internal pressure will fall. The subsequent pressure differential, which depends upon the amount of solar heating which the balloon had experienced, will be reduced, and may, if sufficient gas was expelled, reach zero. As long as the volume remains constant, there will be no change in altitude; however, if ΔP does drop to zero, the volume will start to decrease, and, as described earlier, the equilibrium will not be stable. If the balloon starts to fall, it will continue to fall through the constant-temperature region of the atmosphere. This is because under such circumstances the volume V diminishes at the same rate as the atmospheric density increases, so that the product $V\rho_a$, and therefore the lift force, is constant. As the balloon enters warmer air it will be partially re-inflated and can reach neutral (but not stable) equilibrium.

The maximum tolerable temperature-rise due to solar heating may be obtained by assuming that, as a result of the expulsion of gas, and the subsequent cooling to atmospheric temperature, the pressure differential just drops to zero. Under these conditions, since the volume and the amount of gas contained in the balloon are fixed during the cooling process,

$$\frac{P_a + \Delta P}{T_a + \Delta T} = \frac{P_a}{T_a}, \quad (26)$$

whence

$$\Delta T = \frac{\Delta P}{P_a} T_a \quad (27)$$

Thus the temperature stability factor increases with altitude, and at a given altitude, is proportional to ΔP . ΔT is plotted vs. altitude, for several values of ΔP , in Fig. 5.

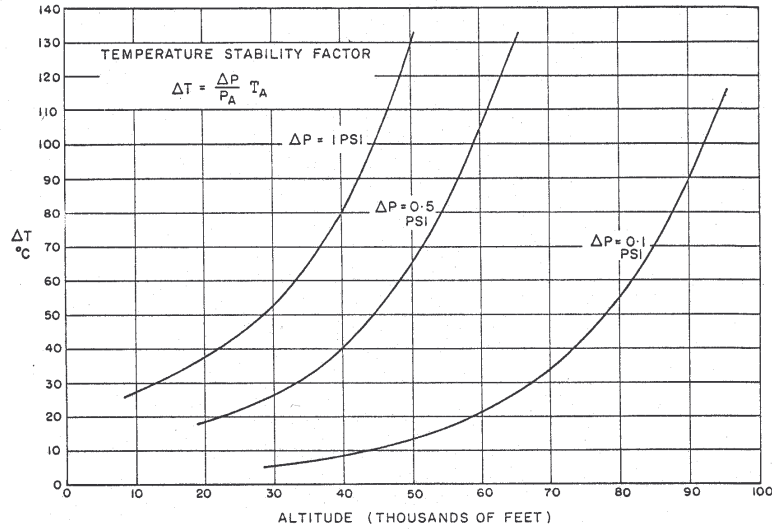


Fig. 5 Temperature stability factor for superpressured balloons

BURSTING STRESS OF SPHERICAL PLASTIC BALLOONS

The allowable ΔP depends upon the rupturing stress of the material. The actual stress is very easily calculated for spherical balloons, while for more complex configurations, e.g., tetrahedrons, empirical formulas must be used.

Consider a thin spherical shell of thickness t , and radius r , which is pressurized ΔP lbs/in² above atmospheric pressure. The total force exerted upon any hemisphere by the gas is $\Delta P \pi r^2$ pounds. This force is transmitted to the other hemisphere by a total cross-sectional area of $2 \pi r t$ square inches of material, so that the stress is given by

$$S = \frac{\Delta P \pi r^2}{2 \pi r t} = \frac{r \Delta P}{2 t} \quad (28)$$

Although this formula is applicable only to ideal, seamless spherical balloons, it is of considerable use in estimating the bursting pressure of actual balloons.

By comparison of (28) with (27), it may be seen that the selection of ΔP requires a compromise between good temperature stability and low stress in the balloon material. Fortunately, at very high altitudes, where large-diameter balloons must be used, good temperature stability is obtained with small values of ΔP , so that the stress does not become excessive.

The pressure differential required to produce a stress of 7500 psi in the balloon material has been plotted in Fig. 6 for various balloon sizes. This stress is approximately 75% of the rupturing stress of Mylar.

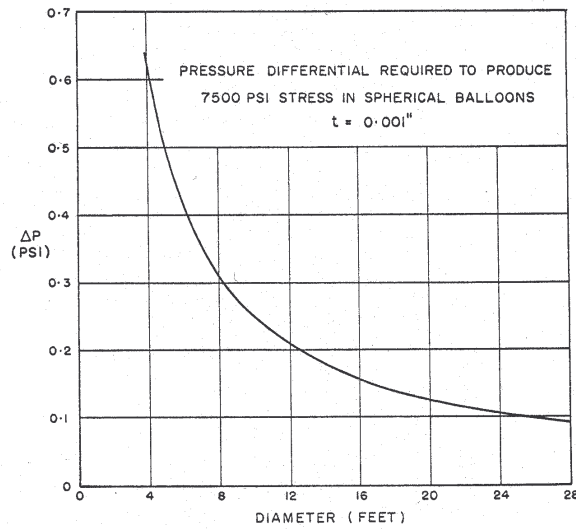


Fig. 6 ΔP versus diameter for 7500 psi stress in 1-mil spherical balloons

RADAR CROSS SECTION AND REFLECTIVITY
OF METALLIZED PLASTIC BALLOONS

The back-scattering cross section of a conducting sphere is dependent upon the ratio a/λ , where a is the radius. The relationship is shown in, for example,

Fig. 2.10 of Skolnik's book, "Introduction to Radar Systems" [1]. From the figure it may be seen that for $a \gg \lambda$, the radar cross section approaches the geometrical cross section πa^2 ; i.e., it is independent of frequency. To make the cross section sensibly independent of wavelength the radius should be chosen so that a/λ exceeds about 1.5 at the lowest frequency of interest. If, however, the radius is made too large, balloon costs increase rapidly, and the maximum free-space range of the balloons may greatly exceed the horizon distance of the radar whose performance is to be evaluated. Under these conditions, a significant degradation in radar performance might occur without any reduction in the detection range on the balloons.

Assuming an effective earth radius of $4/3 R$ for propagation purposes, the radar horizon distance for a target altitude of 40,000 feet is approximately 280 miles. For many surveillance radars the range to be expected on a target having a radar cross section of 1 metre² is 100 to 200 miles; consequently, reflecting balloons 4 feet in diameter have been chosen as the standard target. The geometrical cross section of such a balloon is 1.17 metres². For wavelengths shorter than about 40 cm, this figure is a very good approximation to the radar cross section; consequently these balloons do not suffer from the deficiencies of smaller aluminum spheres which are also used as radar targets [2].

In the calculation of radar cross section it has been assumed that the metallized plastic balloons are perfect conductors. The validity of this assumption was determined by measurements of the reflectivity of samples of various metallized plastics.

Expressions have been published by Koide [3], and by Schneider [4] for the microwave reflectivity of thin metallic films. In the course of this work, an experimental determination of the reflectivity of vacuum-deposited aluminum films and a correlation of reflectivity with the thickness and resistivity of the film has been made.

In an effort to determine the thickness of such films, the d-c resistance of a number of samples was measured. It was observed, however, that for samples whose thicknesses were known to lie in the range 400 to 2000 angstrom units, the resistance considerably exceeded values calculated on the basis of the bulk conductivity of aluminum. This is at variance with evidence presented by Holland [5] who indicates that for films of these thicknesses the bulk conductivity should apply. The discrepancy may possibly be related to the difference in substrates; Holland's reference is to films deposited on glass, while the samples used in these experiments were deposited on plastics.

To resolve this discrepancy, the amount of aluminum per unit area was determined by chemical means. The thickness was then calculated assuming that

the films had the density of bulk aluminum. Table I lists the resistance and thickness data obtained for various samples of metallized plastic. For most of the samples, the measured resistance is $3\frac{1}{2}$ to 4 times that based on the bulk conductivity value.

The reflectivity factors were determined from VSWR measurements made at 3000 mc/s on film samples which were clamped between choke flanges in an RG-48/U waveguide system. The values have been corrected for losses in the waveguide between the probe and the sample.

TABLE I — SUMMARY OF MEASUREMENTS ON ALUMINIZED PLASTICS

Sample No.	Substrate	Ohms/Square	Film Thickness (Å)	Power Reflected (%)
1	Mylar	3.75	252	97.0
2	Mylar	1.55	600	98.6
3	Melinex	1.6	422	98.6
4	Melinex	6.8	329	93.3
5	Melinex	1.8	545	97.6
6	Melinex	4.3	337	97.2
7	Melinex	3.3	370	97.4
8	Mylar	1.0	918	99.2

Using Schneider's Eq. 12, the percentage of incident power reflected by aluminum films having thicknesses between 100 and 1000 angstrom units has been calculated for various values of conductivity, and the results plotted in Fig. 7. Experimentally determined points are included, and it may be seen that, with one exception, the points lie reasonably close to the curve calculated for $\sigma' = 0.25 \sigma_0$. Thus, for films of this type, the effective conductivity to be used in computing reflectivity is about 25% of that of bulk aluminum. In addition, the data of Table I provide a guide for estimating the amount of power reflected, from a measurement of the d-c resistance.

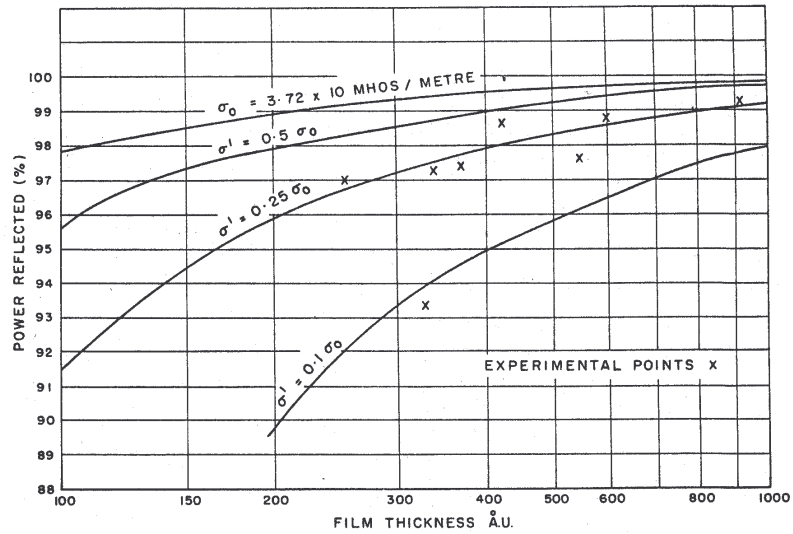


Fig. 7 Calculated reflectivity of aluminum film in RG48/U waveguide at 3.0 Gc/s

FLIGHT CHARACTERISTICS OF VARIOUS BALLOON ASSEMBLIES

The radar target balloons employed in the project were four feet in diameter. Such balloons, when metallized, provided the standard reflecting area required. Used alone, they can attain altitudes of 40 to 55 thousand feet, depending upon the material thickness. For greater altitude, the target balloons are attached to larger lifting balloons. Fig. 8 may be used as a guide in the selection of the appropriate size. This figure shows the maximum equilibrium altitude for Mylar balloons of two different thicknesses when pressurized to 0.1 psi above atmospheric pressure. In the preparation of this figure, it has been assumed that helium is used as the lifting gas, and that the seam factor is 1.20 (i.e., that a 20% allowance for the seams, polar caps, etc. must be made in the computation of the balloon mass, M_B). The mass of the valve, M_V , is 37 grams (measured). M_A has been set equal to zero (i.e., no accessories are carried).

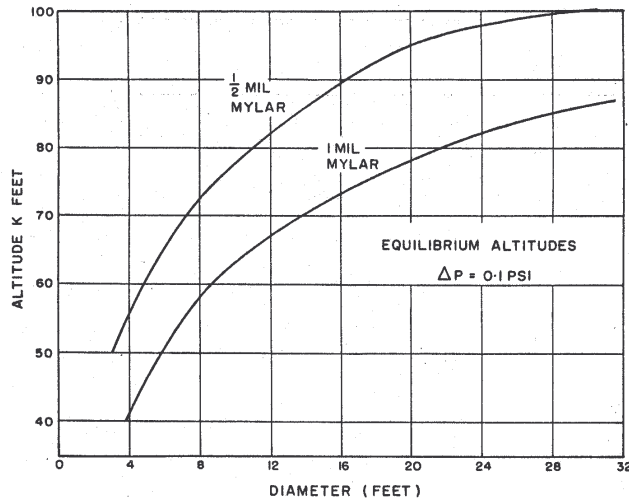


Fig. 8 Calculated equilibrium altitudes for spherical balloons

Balloons fabricated from material thinner than $\frac{1}{2}$ mil are considered impractical for this project because of their fragility. From Fig. 8 it may be seen that, in order to achieve altitudes in excess of 55,000 feet, the balloon diameter must be greater than 4 feet. Since a constant echoing area is desired, unmetallized lifting balloons have been employed to carry the four-foot metallized balloons up to the desired altitude. The equilibrium altitude for the double-balloon case may be obtained using Figs. 1, 2, and 3, provided that ρ_B is computed from

$$\rho_B = \frac{M_B + m_B}{V + v},$$

where the upper and lower case letters refer to the lifting and target balloons, respectively. Although this method of determining the altitude is based on the assumption that both balloons are filled with helium to the same pressure, the error will not be significant if the pressures differ. If the lifting balloon is large, so that $V \gg v$, the target balloon may even be filled with air without causing any appreciable reduction in equilibrium altitude.

The calculated flight characteristics of a number of different balloon configurations appear in Table II. Since solar heating is not expected to exceed 40°C, most of these configurations should be useful.

TABLE II
FLIGHT CHARACTERISTICS OF VARIOUS BALLOON CONFIGURATIONS

Lifting Balloon	Target Balloon	ΔP for 7500 psi stress (psi)	Altitude (night) (ft.)	Altitude (day) (ft.)	Tolerable Solar Heating (°C)
None	4' - 1 mil	0.6	40,500	41,000	48
None	4' - $\frac{1}{2}$ mil	0.3	54,500	55,500	48
8' - 1 mil	4' - 1 mil	0.3	54,500	55,500	48
8' - $\frac{1}{2}$ mil	4' - 1 mil	0.15	65,000	65,500	38
12' - 1 mil	4' - 1 mil	0.20	64,500	65,000	52
12' - $\frac{1}{2}$ mil	4' - 1 mil	0.10	77,500	78,500	47
20' - 1 mil	4' - 1 mil	0.12	76,000	77,000	54
20' - $\frac{1}{2}$ mil	4' - 1 mil	0.06	91,000	93,000	55
25' - 1 mil	4' - 1 mil	0.10	82,000	83,000	60
25' - $\frac{1}{2}$ mil	4' - 1 mil	0.05	98,500	100,000	75

EXPERIMENTAL RESULTS

The operational results obtained by the use of reflecting balloons are reported elsewhere [6]; however, a number of experiments and measurements designed to test the balloons are described below along with a brief summary of the trial results.

Leakage tests were conducted on a number of balloons supplied by different manufacturers. In these tests, the balloons were inflated with a mixture of 90%

SOURCES OF ATMOSPHERIC DATA

- a) "Handbook of Chemistry and Physics", 36 Ed. (The Chemical Rubber Company, Cleveland, Ohio) p. 3093
- b) H.H. Koelle, "Handbook of Astronautical Engineering" (McGraw-Hill Book Company, Inc., New York, N.Y., 1961) pp. 2-5 to 2-9

REFERENCES

1. M.I. Skolnik, "Introduction to Radar Systems", (McGraw-Hill Book Company, Inc., New York, N.Y., 1962)
2. D.K. Barton, "Radar System Analysis", (Prentice-Hall Inc., Englewood Cliffs, N.J., 1964) p. 531
3. F.T. Koide, "Depth of Penetration as a Measure of Reflectivity of Thin Conductive Films", Proc. IRE, vol. 48, pp. 1654-1655, September 1960
4. K.V. Schneider, "Reflection and Transmission of Conductive Films", Proc. IRE, vol. 49, pp. 1090-1091, June 1961
5. L. Holland, "Vacuum Deposition of Thin Films", (John Wiley and Sons, Inc., New York, N.Y., 1956) p. 207
6. J. Akeroyd, "Reflecting Balloons for Radar Evaluation", NRC Report ERB-698, April 1965

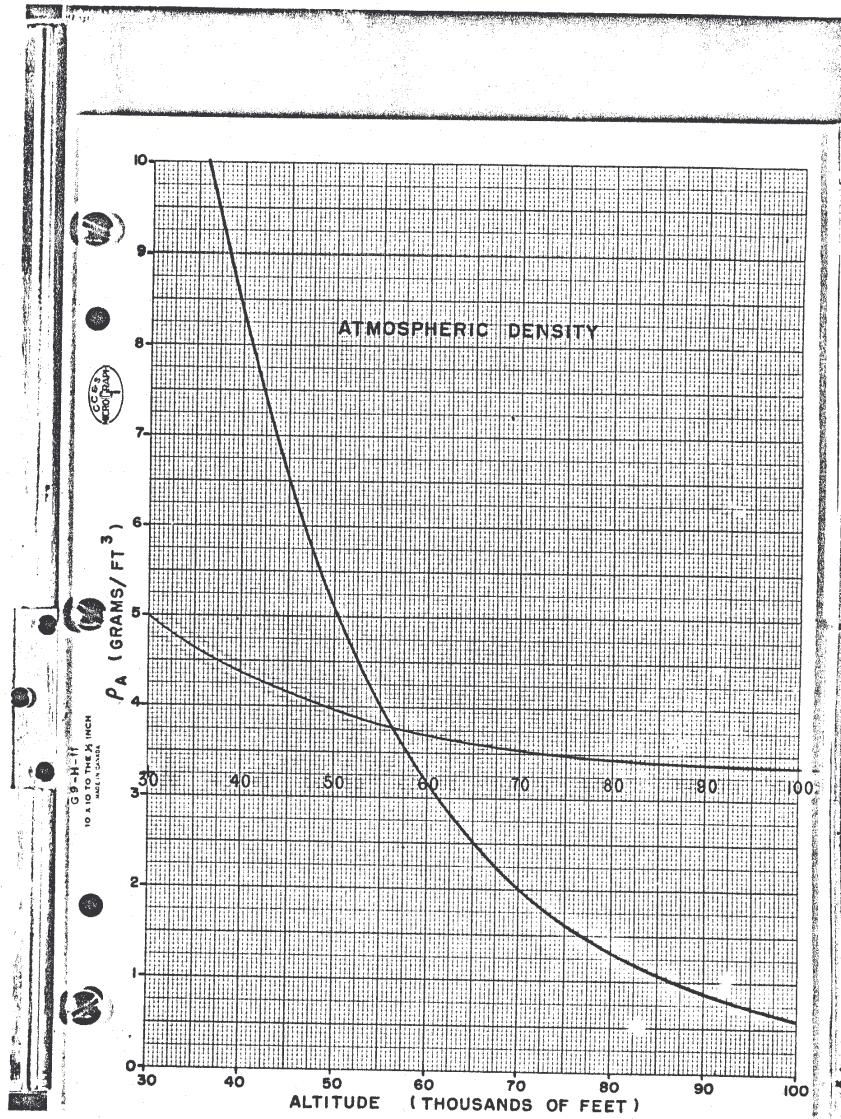


Plate I — Balloon height calculator